International Journal of Mass Spectrometry 294 (2010) 54–58

Contents lists available at ScienceDirect

International Journal of Mass Spectrometry

journal homepage: www.elsevier.com/locate/ijms

Calculations of total and ionization cross-sections on electron impact for alkali metals (Li, Na, K) from threshold to 2 keV

Minaxi Vinodkumar[a,*], Kirti Korot[b], Harshad Bhutadia[a]

[a] V.P. & R.P.T.P. Science College, Vallabh Vidyanagar 388 120, Gujarat, India
[b] Department of Physics, Faculty of Engineering & Technology, Charusat, Changa 388 421, India

ARTICLE INFO

Article history:
Received 6 April 2010
Received in revised form 8 May 2010
Accepted 10 May 2010
Available online 15 May 2010

PACS:
34.80 Bm

Keywords:
Ionization cross-section
Total cross-section
CSP-ic method
SCOP
Alkali atom

ABSTRACT

In this article we report calculations of the total elastic, Q_{el}, total ionization, Q_{ion}, and total (complete), Q_T, cross-sections for the targets Li, Na, K having low ionization thresholds and high polarizability upon electron impact for energies from circa threshold to 2000 eV. We have employed the well-known spherical complex optical potential (SCOP) formalism, which provides total elastic cross-section (Q_{el}) and its inelastic counterpart (Q_{inel}). The sum of Q_{el} and Q_{inel} gives the total (complete) cross-section, Q_T, which is found to be very high at the lower energies (around 5 eV). This is attributed to high polarizabilities and low ionization thresholds of these atoms. Q_{inel} includes Q_{ion} and we have developed a semi-empirical method, called complex scattering potential-ionization contribution (CSP-ic) to extract ionization cross-sections from calculated total inelastic cross-section. Present calculations also provide information on the total excitation processes of these targets. The calculated cross-sections are examined as functions of incident electron energy along with available comparison and overall good agreement is observed.

1. Introduction

The alkali metals are highly reactive and as a consequence are never found in elemental form in nature. Alkaline metals, having the electronic configuration of noble gas atoms with an *s*-electron added, are targets with very high polarizability [1]. Further, they have the lowest ionization potentials in their respective periods, as removing the single electron from the outermost shell give them the stable inert gas configuration. The low ionization potentials of the alkali metals make them useful candidate as sources of quiescent plasmas, their high electric polarizabilities result in large elastic, inelastic and ionization cross-sections, ideal for many applications [2,3]. Moreover it is expected that electron atom scattering studies should provide a common meeting ground for experiment and theory as alkali metal atoms beams are relatively easy to produce and detect and for theoreticians they are effectively one electron system. Due to the cited properties, alkali metals are of obvious interest for both theoreticians and experimentalists [4,5].

Total cross-sections (TCS) for electron scattering from atoms and molecules provide useful insight in verifying and testing various models of electric and magnetic interactions. Electron-induced ionization cross-sections and probabilities of other processes like excitations in atoms/molecules determine the density and reactivity of low temperature technological plasmas. Along this line of investigation, the electron as well as positron induced processes, including ionization as a dominant inelastic channel at intermediate and high energies, play important roles in plasma-processing, aeronomy and in biological systems and other environmental sciences. Moreover, in order to develop understanding of the basic chemical behavior of above listed alkali atoms (Li, Na, K), the data regarding the total elastic, inelastic and ionization cross-sections would prove crucial and therefore such study has attracted many theoreticians and experimentalists in last few decades. Here we are interested in the intermediate and high-energy region (from ionization threshold up to 2 keV) where almost all inelastic channels are open.

Theoretical calculations as well as experimental studies [3,6] of TCS, Q_T, for Li are scarce. This scarcity of experimental work is due to lower vapor pressure of Li gas. Lower vapor pressure requires hot sources and hot lithium vapor is very corrosive, and lithium atoms are more difficult to detect than the other alkalis [6]. Jaduszliwer et al. [6] have reported Q_T with the atomic-recoil technique and Kasdan et al. [3] have measured Q_T using modified Ramsauer technique. For Q_{ion} there are good experimental investigations [7,8], but theoretical data is reported only by McFarland [9] using classical theory of Gryzinski. McFarland and Kinney [7] and Brink [8] have reported measured Q_{ion} with the help of crossed beam technique.

For sodium, against only one theoretical data of Walters [10], there is large number of experimental data reported by [3,11,12] for Q_T. The theoretical data of Walters [10] is obtained by adding the cross-sections from existing theoretical results for elastic,

* Corresponding author. Tel.: +91 2692 230011.
E-mail address: minaxivinod@yahoo.co.in (M. Vinodkumar).

1387-3806/$ – see front matter © 2010 Elsevier B.V. All rights reserved.
doi:10.1016/j.ijms.2010.05.010

resonance excitation, and the sum of all other discrete excitations, and from existing experimental results for the ionization cross-sections. Kasdan et al. [3] used atomic-recoil technique. Srivastava and Vuskovic [11] used crossed-electron-beam-metal-atom-beam scattering technique and Kwan et al. [12] used beam-transmission technique respectively to measure the total (complete) cross-section for e–Na system. Q_{ion} for Na is calculated by Huang et al. [13] with the help of binary–encounter–bethe (BEB) model. The experimental total ionization cross-sections for Na are reported by McFarland and Kinney [7] and Brink [8].

For potassium, Q_T is experimentally measured by many groups in different ranges of incident energies [3,12,14–17]. Kasdan et al. [3] used atomic-recoil technique, Kwan et al. [12] and Stein et al. [14] used beam-transmission technique, Visconti et al. [15] used atom-beam recoil technique, Vuskovic and Srivastava [16] used crossed-electron-beam-metal-atom-beam scattering technique and Brode [17] used atom-beam recoil technique to measure the electron impact total cross-sections for potassium. While theoretically results for Q_T are reported by only two groups, Walter [10] and Gein [18]. The theoretical results of Gein [18] were obtained by employing the modified Glauber approximation within the model potential approach. Total ionization cross-sections, Q_{ion}, are measured by two experimental groups, McFarland and Kinney [7] and Brink [8]. The theoretical data of ionization cross-sections for potassium is reported only by McFarland [9].

Presently we have made use of the well-established complex optical potential (SCOP) to evaluate total elastic, inelastic and ionization cross-sections. The methodology employed is discussed in the next section depicting the salient features of the theory. A more detailed description can be found in our earlier papers [19–24].

2. Theoretical methodology

Depending on the energy of the incident projectile, all the processes resulting from the interaction of incoming projectile with target can be broadly classified into elastic and inelastic processes. The energy of present interest is from ionization threshold of the target to 2000 eV. The total cross-section can be expressed as sum of total elastic and total inelastic cross-sections as

$$Q_T(E_i) = Q_{el}(E_i) + Q_{inel}(E_i) \tag{1}$$

We have employed well-known spherical complex optical potential (SCOP) formalism to evaluate the cross-sections given vide Eq. (1) and has been found to be very successful for intermediate- and high-energy collisions. All the total cross-sections are derived from complex potential that is developed between the projectile and the target. The complex optical potential, V_{opt}, thus consists of real as well as imaginary parts given by

$$V_{opt}(E_i, r) = V_R(E_i, r) + iV_I(E_i, r) \tag{2}$$

Here, the second term is usually considered as an "absorption effect" and it is phenomenologically represented by an imaginary potential. While the first term is the real potential which takes into account the static, exchange and the polarization effects. Static and exchange effects are short-range potentials while polarization is a long range potential. Hence, we represent the real potential as

$$V_R(E_i, r) = V_{st}(r) + V_{ex}(E_i, r) + V_P(E_i, r) \tag{3}$$

All these potentials are functions of the electronic charge density of the target which is derived from the Hartree Fock wave functions of Bunge et al. [25]. For the exchange potential, we have used Hara's 'free electron gas exchange model' [26]. And for the polarization potential, V_p, we have used parameter free model of correlation-polarization potential given by Zhang et al. [27]. The present model contains some multipole non-adiabatic corrections in the intermediate region and it smoothly approaches the correct asymptotic form at large 'r'.

The imaginary part V_I in Eq. (2), also called the absorption potential, V_{abs}, accounts for the total loss of scattered flux into all the allowed channels of electronic excitation and ionization. For V_{abs}, we have used the model potential given by Staszeweska et al. [28], which is a non-empirical, quasifree, Pauli-blocking, dynamic absorption potential. The form of the potential is given as

$$V_{abs}(r, E_i) = -\rho(r)\sqrt{\frac{T_{loc}}{2}}\left(\frac{8\pi}{10k_F^3 E_i}\right)\theta(p^2 - k_F^2 - 2\Delta)(A_1 + A_2 + A_3) \tag{4}$$

The local kinetic energy of the incident electron is given by

$$T_{loc} = E_i - (V_{st} + V_{ex}) \tag{5}$$

The absorption potential is not sensitive to long range potentials like V_{pol}. In Eq. (4), $p^2 = 2E_i$, $k_F = [3\pi^2\rho(r)]^{1/3}$ is the Fermi wave vector and Δ is an energy parameter. Further $\theta(x)$ is the Heaviside unit step-function, such that $\theta(x) = 1$ for $x \geq 0$, and is zero otherwise. The dynamic functions A_1, A_2 and A_3 occurring in Eq. (4) depend differently on $\rho(r)$, I, Δ and E_i. The explicit forms of A_1, A_2 and A_3 can be found in earlier paper [19]. The energy parameter Δ determines a threshold below which $V_{abs} = 0$, and the ionization or excitation is prevented energetically. We have modified the original model, by considering Δ as a slowly varying function of E_i around I. Necessity for such modification has been also discussed by Blanco and Garcia [29]. Briefly, a preliminary calculation is done with a fixed value $\Delta = I$, but Δ as a variable accounts for the screening of the absorption potential in the target charge-cloud region. Further this is meaningful since Δ fixed at I would not allow excitation at incident energy $E_i \leq I$. On the other hand, if parameter Δ is much less than the ionization threshold, then V_{abs} becomes significantly high near the peak position which is unphysical. After generating the full complex potential given in Eq. (2) for a given electron–atom system, we solve the Schrödinger equation numerically and use partial wave analysis to get complex phase shifts which are the key ingredients to find the relevant cross-sections.

The total inelastic cross-sections, Q_{inel}, cannot be measured directly in experiments; however it can be estimated by subtracting total integral elastic cross-section from the measured grand total cross-sections. The measurable quantity of applied interest is the total ionization cross-section, Q_{ion}, which is contained in the Q_{inel}. The Q_{inel} can be partitioned into discrete and continuum contributions, viz.,

$$Q_{inel}(E_i) = \sum Q_{exc}(E_i) + Q_{ion}(E_i) \tag{6}$$

where the first term is the sum over total excitation cross-sections for all accessible electronic transitions. The second term is the total cross-section of all allowed ionization transitions to continuum induced by the incident electrons. The first term arises mainly from the low-lying dipole allowed transitions for which the cross-section decreases rapidly at higher energies. The first term in Eq. (6), therefore becomes progressively smaller than the second at energies well above the ionization threshold. By definition,

$$Q_{inel}(E_i) \geq Q_{ion}(E_i) \tag{7}$$

This is an important inequality and forms basis of our CSP-ic method. However, Q_{ion} cannot be rigorously derived from Q_{inel} but may be estimated by defining the energy dependent ratio of cross-sections,

$$R(E_i) = \frac{Q_{ion}(E_i)}{Q_{inel}(E_i)} \tag{8}$$

such that, $0 < R \lesssim 1$.

We require $R = 0$ when $E_i \leq I$. This is an exact condition as the ionization channel opens up only when incident energy of projectile is greater than ionization threshold of the target implying that the ionization cross-sections will be zero for $E_i < I$. For a number of stable atoms and molecules like Ne, O_2, H_2O, CH_4, SiH_4, etc., for which the experimental ionization cross-sections, Q_{ion}, are known accurately [30,31] the ratio R rises steadily as the energy increases above the threshold, and approaches unity at high energies. Thus, we can summarize these physical arguments in the form of mathematical equations as

$$\begin{aligned} R(E_i) &= 0 \quad \text{for } E_i \leq I \\ &= R_P \quad \text{at } E_i = E_P \\ &\cong 1 \quad \text{for } E_i >> E_P \end{aligned} \tag{9}$$

where 'E_p' stands for the incident energy at which the calculated Q_{inel} attains its maximum value. R_p is the value of R at $E_i = E_p$.

Perhaps a first ever estimate of ionization in relation to excitation processes was made by Turner et al. [32]. They concluded from semi-empirical calculations that in gaseous water (H_2O), ionization was more probable than excitation above ~30 eV. If σ_{ion} and σ_{exc} are the cross-sections of ionization and excitation respectively then almost above 100 eV,

$$\frac{\sigma_{ion}}{\sigma_{ion} + \sigma_{exc}} \approx 0.75 \tag{10}$$

It is to be noted that ratio given in Eq. (10) resembles the one defined by us in Eq. (8). The general observation is that, at energies close to peak of ionization, the contribution of Q_{ion} is about 70–80% of the total inelastic cross-sections, Q_{inel}. For consistency of our method, for all the targets we have chosen $R_p \approx 0.7$. For calculating the Q_{ion} from Q_{inel} we need R as a continuous function of energy for $E_i > I$; hence we represent the ratio R in the following manner,

$$R(E_i) = 1 - f(U) \tag{11}$$

Presently the above ratio has been determined using the following analytical form [19–24].

$$R(E_i) = 1 - C_1 \left(\frac{C_2}{U + a} + \frac{\ln(U)}{U} \right) \tag{12}$$

where U is the dimensionless variable defined by, $U = E_i/U$.

The reason for adopting a particular functional form of $f(U)$ in Eq. (12) is as follows. As E_i increases above I, the ratio R increases and approaches 1, since the ionization contribution rises and the discrete excitation term in Eq. (6) decreases. The discrete excitation cross-sections, dominated by dipole transitions, fall off as $\ln(U)/U$ at high energies. Accordingly the decrease of the function $f(U)$ must also be proportional to $\ln(U)/U$ in the high range of energy. However, the two-term representation of $f(U)$ given in Eq. (12) is more appropriate since the first term in the brackets ensures a better energy dependence at low and intermediate E_i. The dimensionless parameters C_1, C_2, and a, involved in Eq. (12) reflect the properties of the target under investigation. The three conditions stated in Eq. (9) are used to determine these three parameters. This method is called the complex scattering potential-ionization contribution, (CSP-ic). Having obtained Q_{ion} through CSP-ic, the summed excitations cross-sections $\sum Q_{exc}$ can be easily calculated vide Eq. (6). However the values of $\sum Q_{exc}$ for all these targets are not reported here but are available with the authors.

3. Results

The theoretical approach of SCOP along with our CSP-ic method discussed above allows us to determine the various total cross-sections Q_T, Q_{el} and Q_{ion} along with the useful estimation of

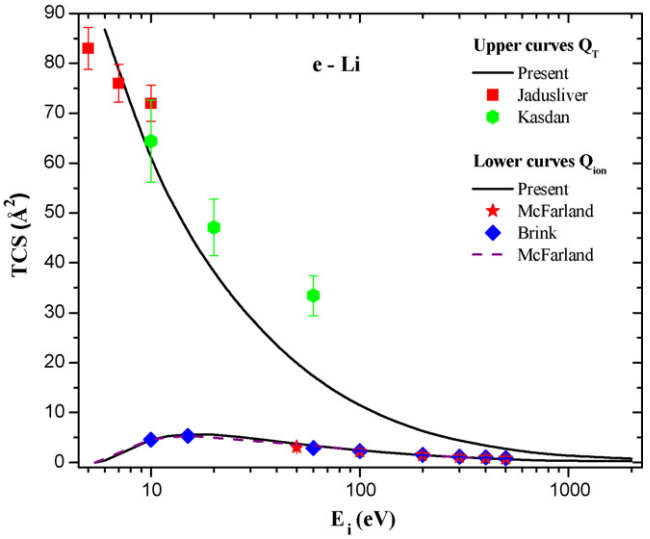

Fig. 1. Total (complete) cross-sections and total ionization cross-sections for e–Li scattering in Å^2. Upper curves: solid line, present Q_{ion}; hexagons, Kasdan et al. [3]; rectangles, Jaduszliwer et al. [6]. Lower curves: solid line, present Q_{ion}; stars, McFarland and Kinney [7]; squares, Brink [8] and dashed line, McFarland [9].

electronic excitations in terms of the summed cross-section $\sum Q_{exc}$. The present results for the total (complete) cross-sections and total ionization cross-sections for alkali atoms (Li, Na, K) are plotted in Figs. 1–3. Total ionization cross-sections are calculated using the CSP-ic method. Motivation for this study was to check the consistency of our CSP-ic method for a set of special targets which have low ionization threshold and high polarizability. Inspection of the results and the comparison with available data makes us more confident to apply the methodology to still more complex systems.

Fig. 1 shows comparison of the total (complete) cross-sections and total ionization cross-sections for e–Li scattering. There is scarcity of data and first time the data of the total (complete) cross-sections has been reported over such a wide range (threshold to 2 keV). There are no theoretical data for comparison of total cross-section. The total (complete) cross-sections are very large in magnitude at the lower energies. This can attributed to two properties

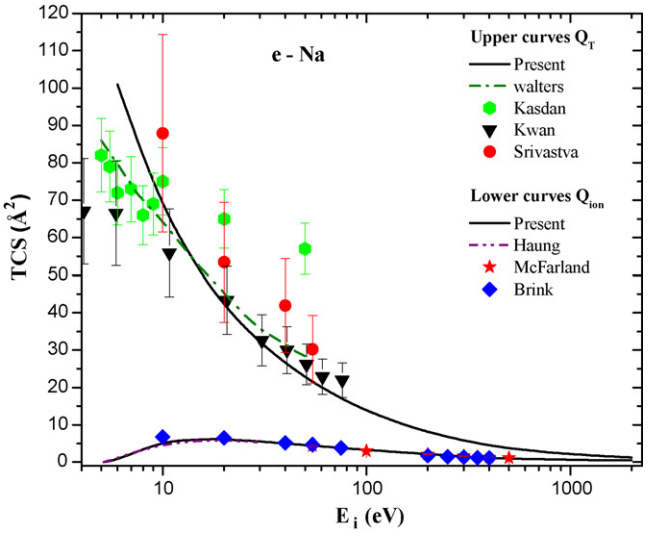

Fig. 2. Total (complete) cross-sections and total ionization cross-sections for e–Na scattering in Å^2. Upper curves: solid line, present Q_{ion}; circles, Srivastva and Vuskovic [11]; triangles, Kwan et al. [12]; hexagons, Kasdan et al. [3]; dashed dot line, Walters [10]. Lower curves: solid line, present Q_{ion}; dashed dot dot line, Huang et al. [13]; stars, McFarland and Kinney [7]; squares, Brink [8].

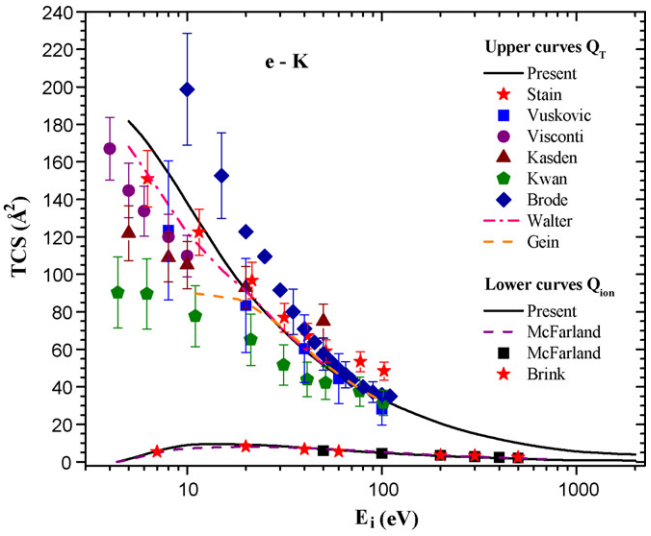

Fig. 3. Total (complete) cross-sections and total ionization cross-sections for e–K scattering in Å^2. Upper curves: solid line, present Q_{ion}; stars, Stain et al. [14]; rectangles, Vuskovic and Srivastva [16]; circles, Visconti et al. [15]; triangles, Kasdan et al. [3]; pentagons, Kwan et al. [12]; squares, Brode [17]; dashed dot line, Walters [10]; dashed line, Gein [18]. Lower curves: solid line, present Q_{ion}; rectangles, McFarland and Kinney [7]; stars, Brink [8]; dashed line, McFarland [9].

of target, viz., low ionization threshold and high polarizability. The present results compare well with the available experimental values of Kasdan et al. [3] and Jadusliwer et al. [6] at low energies below 30 eV. The lower curves are for the total ionization cross-sections. They are compared with previous theoretical data of McFarland [9] and the experimental data of McFarland and Kinney [7] and Brink [8]. The present results are in very good accord with theoretical values of McFarland [9] for entire energies reported by them except around peak value. At peak the present results are slightly higher than results of McFarland [9]. The experimental results of McFarland and Kinney [7] and Brink [8] are also in very good accord with present data for the entire energy range. Also, the shape of the cross-section curve is almost the same for both the theoretical results.

Fig. 2 shows our calculations for the total (complete) cross-sections and total ionization cross-sections for e–Na scattering with comparison. As seen in previous case, the total cross-sections are very high at the lower energies because of its high polarizability and low ionization threshold. The present results are in excellent agreement with the experimental values of Kwan et al. [12] at higher energies but are higher compared to them at low energy. The present results are also compared with the experimental investigations of Srivastva and Vuskovic [11] and their values are higher than present data throughout the range reported by them. The experimental results of Kasdan et al. [3] are fairly good with present results at lower energies but go high at higher energies. The only available theoretical investigation in the literature is Walters [10] and they show good agreement with present data beyond 10 eV below which the present data is high. It is to be noted that there is remarkable difference in the data obtained through different experiments. The lower curves in Fig. 2 show comparison of the total ionization cross-sections for electron impact on Na with available data. The present results are in very good accord with theoretical values of Huang et al. [13] at low energies and are only slightly higher around the peak value. The experimental results of McFarland and Kinney [7] and Brink [8] are also very good accord with present data in entire energy range except first few experimental data point.

Fig. 3 shows our calculations of the total (complete) cross-sections and total ionization cross-sections for e–K scattering along with available comparison. Potassium is more widely studied experimentally. As in the case of sodium for this target also a large variation is seen in the data for different experimental groups [3,12,14–17]. The present results are compared with available experimental results [3,12,14–17] and theoretical results [10,18]. Our data goes from the centre of all reported values throughout the energy range. Beyond 30 eV all data are in good accord with present reported values but below it there is large variation. The experimental values of Stein et al. [14] are in good accord throughout the range specified by them. The measured values of Vuskovic and Srivastava [16] are much higher than all reported values below 30 eV. The measured values of Visconti et al. [15] and Kasden et al. [3] are lower compared to present data below 30 eV. The experimental data of Kwan et al. [12] are the lowest compared to all reported data. The theoretical results of Walters [10] and Gein [18] are in very good agreement with present data beyond 20 eV. In Fig. 3 we also compare the total ionization cross-section for e–K scattering with available data. Only one theoretical data [9] and two experimental data [7,8] are found in the literature. The present results are slightly higher than all the available results near the peak region but at low- and high-energy regime overall good agreement is seen. The theoretical results of McFarland [9] are in very good accord with present data throughout the energy regime except at the peak where they are lower than the present data. The experimental results of McFarland and Kinney [7] and Brink [8] are also overall good accord with present data in entire energy range except peak region.

This study is meaningful since there is no theoretical data available for these targets beyond 100 eV. Moreover a large discrepancy is seen among various experimental groups and in such situation the comparison with theory becomes important.

4. Conclusion

Electron impact total elastic and total inelastic cross-sections have been calculated for the alkali atoms (Li, Na, K) using the well-known spherical complex optical potential method. The total (complete) cross-section serves as an upper limit to all the cross-sections as it includes all the scattering processes. The complex scattering potential-ionization contribution formalism developed by the authors [19–24] was used to derive the total ionization cross-section for these targets. This method has been tested successfully for a large number of atomic and molecular targets. The derived theoretical total inelastic cross-section serves as the upper limit and gives a useful estimate of the total ionization cross-section. We note that in view of the approximations made here, no definitive values are claimed, but by and large our results fall well within the experimental error in most of the cases. The main advantage of the present method is that all the cross-sections (Q_{el}, Q_{inel}, Q_T, Q_{ion}) calculated here are obtained under the same formalism of SCOP. The present theoretical results for the total (complete) and total ionization cross-sections show good agreement with most of other theoretical and experimental investigations.

Acknowledgments

MVK thankful to University Grants Commission, New Delhi, for Major Research project under which part of this work is done. MVK is also thankful to Department of Science and Technology, New Delhi for funding the major research project.

References

[1] A. Zecca, G.P. Karwasz, R.S. Brusa, Riv. Nuovo Cimento 19 (3) (1996) 1.
[2] K. Nagesha, K.B. MacAdam, Phys. Rev. Lett. 91 (2003) 113202–113211.
[3] A. Kasdan, T.M. Miller, B. Bederson, Phys. Rev. A 8 (1973) 1562.
[4] T.M. Miller, B. Bederson, Adv. At. Mol. Phys. 13 (1977) 1.
[5] E.W. McDaniel, Atomic collisions: Electron and photon projectiles, Wiley, New York, 1989.

[6] B. Jaduszliwer, A. Tino, B. Bederson, T.M. Miller, Phys. Rev. A 24 (1981) 1249.
[7] R.H. McFarland, J.D. Kinney, Phys. Rev. 137 (1965) A1058.
[8] G.O. Brink, Phys. Rev. 127 (1962) 1204.
[9] R.H. McFarland, Phys. Rev. 139 (1965) A40.
[10] H.R.J. Walters, J. Phys. B: At. Mol. Opt. Phys. 9 (1976) 227.
[11] S.K. Srivastava, L. Vuskovic, J. Phys. B: At. Mol. Opt. Phys. 13 (1980) 2633.
[12] C.K. Kwan, W.E. Kauppila, R.A. Lukaszew, S.P. Parikh, T.S. Stein, Y.J. Wan, M.S. Dababneh, Phys. Rev. A 44 (1991) 1620.
[13] J. Huang, T. Furukawa, K. Aoto, M. Yamawaki, J. Mass. Spectrom. Soc. Jpn. 50 (2002) 296.
[14] T.S. Stein, R.D. Gomez, Y.–F. Hsieh, W.E. Kauppila, C.K. Kwan, Y.J. Wan, Phys. Rev. Lett. 55 (1985) 488.
[15] P.J. Visconti, J.A. Slevin, K. Rubin, Phys. Rev. A 3 (1971) 1310.
[16] V. Vuskovic, S.K. Srivastava, J. Phys. B: At. Mol. Opt. Phys. 13 (1980) 4849.
[17] R.B. Brode, Phys. Rev. 34 (1929) 673.
[18] T.T. Gein, J. Phys. B: At. Mol. Opt. Phys. 22 (1989) L129.
[19] M. Vinodkumar, C. Limbachiya, H. Bhutadia, J. Phys. B: At. Mol. Opt. Phys. 43 (2010) 015203.
[20] M. Vinodkumar, C. Limbachiya, B. Antony, K.N. Joshipura, J. Phys. B: At. Mol. Opt. Phys. 40 (2007) 3259.
[21] M. Vinodkumar, K. Korot, C. Limbachiya, B. Antony, J. Phys. B: At. Mol. Opt. Phys. 41 (2008) 245202.
[22] M. Vinodkumar, K.N. Joshipura, C. Limbachiya, N. Mason, Phys. Rev. A 74 (2006) 022721.
[23] M. Vinodkumar, C. Limbachiya, K. Korot, K.N. Joshipura, Euro. Phys. J. D 48 (2008) 333.
[24] M. Vinodkumar, C. Limbachiya, K. Korot, K.N. Joshipura, N. Mason, Int. J. Mass Spectrom. 273 (2008) 145.
[25] C.F. Bunge, J.A. Barrientos, A.V. Bunge, At. Data Nucl. Data Tables 53 (1993) 113.
[26] S. Hara, J. Phys. Soc. Jpn. 22 (1967) 710.
[27] X. Zhang, J. Sun, Y. Liu, J. Phys. B: At. Mol. Opt. Phys. 25 (1992) 1893.
[28] G. Staszewska, D.W. Schwenke, D. Thirumalai, D.G. Truhlar, Phys. Rev. A 28 (1983) 2740.
[29] F. Blanco, G. Garcia, Phys. Rev. A 67 (2003) 022701.
[30] G.P. Karwasz, R.S. Brusa, A. Zecca, Riv. Nuovo Cimento 24 (**1**) (2001) 1.
[31] E. Krishnakumar, S.K. Srivastava, J. Phys. B 21 (1988) 1055.
[32] J.E. Turner, H.G. Paretzke, R.N. Hamm, H.A. Wright, R.H. Richie, Radiat. Res. 92 (1982) 47.